Egypt. J. Chem. **Vol. 66**, No. SI: 13 pp. 1555 - 1561 (2023)

Egyptian Journal of Chemistry

http://ejchem.journals.ekb.eg/

Pushing the Boundaries of Diversity: Innovative Design and Synthesis of Hydrazone-Based Dynamic Combinatorial Libraries of Macrocycles

Amal F. Seliem*

Department of Chemistry, College of Science and Arts, Najran University, P.O. Box 1988, Najran 11001, Saudi Arabia

Abstract

Dynamic combinatorial chemistry (DCC) has emerged as a versatile approach for generating and discovering materials with diverse applications. Utilizing acylhydrazone formation, we developed new dynamic combinatorial libraries (DCLs) of macrocycles and open-structured compounds with intriguing diversity. The DCL constituents were generated *via* condensation reactions using functionalized dihydrazides and aldehydes. Time-of-flight mass spectrometry (TOF-MS) was employed to analyze the library constituents, showcasing its great potential for characterizing DCLs generated by DCC. Our findings highlight the effectiveness of TOF-MS in verifying and validating complex macrocycles generated in solution, making it a valuable technique for discovering new materials through identification and validation of DCLs.

Keywords: Dynamic combinatorial chemistry; dihydrazide; dialdehyde; cyclocondensation; TOF-MS

1. Introduction

Dynamic combinatorial chemistry (DCC) is a powerful synthetic approach that involves the generation of dynamic combinatorial libraries (DCLs) under thermodynamic control [1]. The reversible interactions between the building block constituents of DCLs lead to the generation of a diverse and complex set of products by exploring all possible combinations [2]. This results in the generation of a complex pool of products, making DCC an effective method for the discovery of novel compounds [3]. One of the most significant advantages of DCC over traditional combinatorial chemistry is the ability of DCLs to respond to external stimuli [4]. This unique feature allows for the selective amplification of the constituent that is best suited to respond to the applied stimulus, resulting in the shifting of equilibrium in favor of that constituent as demonstrated in **Figure 1** [5]. Compounds possessing functional groups that are capable of reacting with each other to form reversible bonds are highly advantageous for the generation of DCLs. Functional groups such as imine [6], hydrazone [7], acylhydrazone [8], and disulfide [9] are examples of such groups that can form reversible bonds. The utilization of acylhydrazone-based DCLs has facilitated the discovery of potent compounds, such as cholesterol esterase [10], acetylcholinesterase [11], urease [12], α-amylase [13], 1-deoxy-D-xylulose-5-phosphate synthase [14], and RAD51 [15] inhibitors. More recently, living cells have been employed as templates for achieving targeted amplifications in DCLs [16].

Gawroński and coworkers reported the synthesis of [2+2]-cyclocondensation macrocycles by reacting acetal protected chiral dicarbohydrazides with terephthalaldehyde [17]. The resulting macrocycles comprised four amide functional groups, including two *cis*- and two *trans*-bonds as evidenced by the reported X-ray crystallographic analysis, whereas the trans-bonds were nicely engaged in hydrogen bonding with water molecules [17]. Inspired by this pioneering work, we describe in this study the successful generation of a DCL consisting of macrocycles and open-structured compounds *via* acylhydrazone formation through DCC. The constituents of the DCL were screened by direct injection using atmospheric pressure chemical

*Corresponding author e-mail: afsaleem@nu.edu.sa.;(Amal F. Seliem).
EJCHEM use only: Received date 08 August 2023; revised date 27 August 2023; accepted date 27 August 2023
DOI: 10.21608/EJCHEM.2023.228100.8399

ionization time-of-flight mass spectrometry (APCI-TOF-MS), which provides high sensitivity with non-fragmentation of analytes [18].

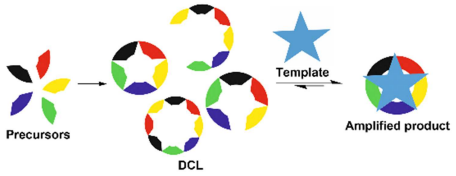

Figure 1. Graphical illustration demonstrating molecular amplification in DCC.

2. Results and Discussion

Synthesis and Characterization

Chiral dihydrazides **3** and **5** were prepared following the stepwise synthetic strategy outlined in **Scheme 1**. In the first step, the carbonyl groups of *N*-substituted-piperidin-4-ones **1** and **4** were protected by the vicinal hydroxyl groups of (+)-diethyl *L*-tartrate **2** using $BF_3(OEt)_2$. In the second step, excess hydrazine hydrate was added to the protected esters, which were then refluxed in absolute ethanol after the basic aqueous workup. The desired products **3** and **5** were obtained in yields of 40% and 45%, respectively. Dihydrazide **7** was prepared following the literature method [19]. The ^{1}H NMR spectrum of compound **3** showed the piperidyl and the methylenic (CH_3CH_2) protons at δ 2.3-1.6 ppm. The dioxolane C*H* appeared at δ 4.4 ppm. The carbohydrazide carbonyl signal appeared in the ^{13}C NMR spectrum at δ 167.7 ppm, while the dioxolane methine signal was observed at δ 76.9 ppm. The characteristic signals of the spiro-piperidy and C=O hydrazide carbon groups appeared in the ^{13}C NMR spectrum at δ 111.3 and 167.7 ppm, respectively. The high-resolution TOF-MS spectrum of compound **3** showed the expected molecular ion peak at *m*/*z* 310.1474 as $[M+Na]^+$.

The chemical structure of compound **5** was verified by ^{1}H NMR through the appearance of the signals of dioxolane C*H* signal at δ 4.5 ppm. The benzyloxy CH_2 group appeared at δ 5.0 ppm, while the piperidy CH_2 groups were observed as multiplet signals at δ 3.3-3.6 and 1.5-1.8 ppm. The ^{13}C NMR spectrum of compound **5** displayed two characteristic signals of the carbohydrazide and carboxylate carbonyl groups at δ 167.6 and 154.8 ppm, respectively. The spiro-piperidy, dioxolane C*H*, C=O carboxylate, and C=O hydrazide carbon signals appeared in the ^{13}C NMR of dihydrazide **5** at δ 110.8, 76.9, 154.8, 167.6 ppm, respectively. The TOF-MS spectrum of compound **5** in the positive ion mode displayed the expected molecular ion peak at *m*/*z* 416.1556 as $[M+Na]^+$.

The ^{1}H NMR spectrum of derivative **7** showed the signal of the dioxolane C*H* group at δ 4.4 ppm. It also displayed the signals of the methyl and methylene groups of the ester functional motif at δ 1.3 and 3.9-4.0 ppm, respectively. The signals of the piperidy CH_2 groups appeared at δ 1.5-1.7 and 3.3-3.4 ppm. The ^{13}C NMR spectrum of **7** showed the characteristic signals of the spiro-piperidyl, dioxolane C*H*, C=O carboxylate, and C=O hydrazide carbons at δ 110.9, 77.2, 155.0, 167.6 ppm, respectively. The chemical structure of dihydrazide **7** was further verified by TOF-MS by the appearance of the expected molecular ion peak in the negative ion mode at *m*/z 330.1419.

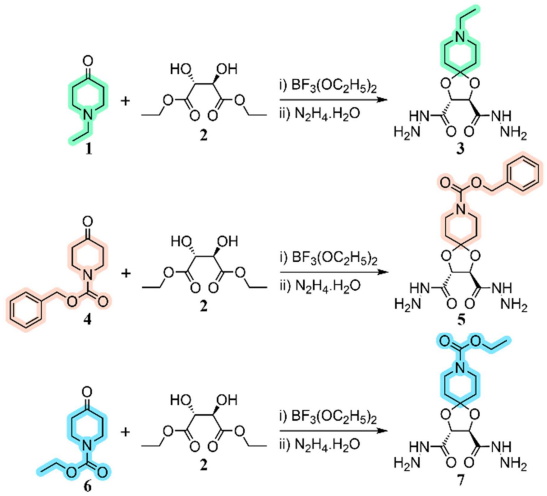

Scheme 1. Synthetic pathway of dihydrazide derivatives **3**, **5**, and **7**.

After successfully synthesizing and analyzing the functionalized dihydrazide precursors **3**, **5**, and **7**, we shifted our focus towards generating the DCLs. The dihydrazides **3**, **5**, and **7** were reacted with terephthalaldehyde **8** in a solution of DMF and MeOH (1: 1) in the presence of AcOH as a catalyst. The reaction mixture was stirred at room temperature for 46 hours, resulting in the formation of an unprecedented DCL of macrocycles **9-11** and open-structured derivatives **12-14**, as depicted in **Scheme 2**. The APCI-TOF-MS spectra of the DCL in the positive ion mode afforded peaks at *m*/*z* 877.3650, 943.3372, 815.3506, 779.3456, 717.3303, and 673.3402, corresponding to the library members **9**, **10**, **11**, **12**, **13**, and **14**, respectively (**Figure 2** and **Table 1**). Intermediates **12-14** were detected after 2 hours of the reaction, while the macrocycles **9-11** were observed after 46 hours. After conducting the reaction for more than 46 hours, we observed that the composition of the DCL remained unchanged, indicating that the reaction had reached a state of equilibrium with maximum stability. As a result, any

further reaction time would not result in significant changes to the composition of the DCL.

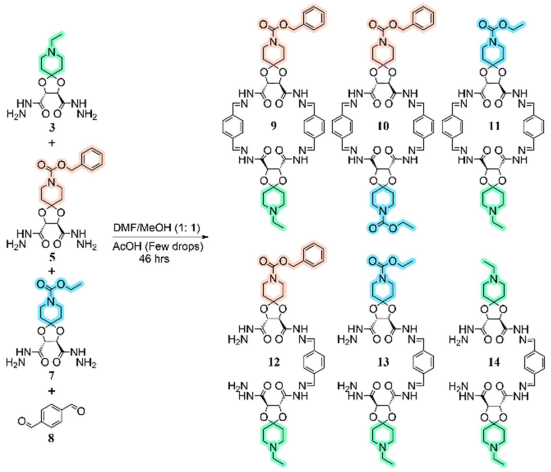

Scheme 2. Generation of a DCL of macrocycle and intermediates **9**-**14**.

Table 1. APCI-TOF-MS data of the DCL members in the positive ion mode

Entry	Molecular Formula	Calcd. *m/z*	Meas. *m/z*		Error ppm
9[a]	$C_{44}H_{49}N_{10}O_{10}$	877.3628	877.3650	$[M+H]^+$	–2.6
10[a]	$C_{45}H_{48}N_{10}NaO_{12}$	943.3345	943.3372	$[M+Na]^+$	–2.9
11[a]	$C_{39}H_{47}N_{10}O_{10}$	815.3471	815.3506	$[M+H]^+$	–4.2
12[b]	$C_{36}H_{47}N_{10}O_{10}$	779.3471	779.3456	$[M+H]^+$	2.0
13[b]	$C_{31}H_{45}N_{10}O_{10}$	717.3315	717.3303	$[M+H]^+$	1.6
14[b]	$C_{30}H_{45}N_{10}O_8$	673.3416	673.3402	$[M+H]^+$	2.1

[a]Detected after 46 hours and [b]detected after 2 hours of stirring at room temperature

The APCI-TOF-MS spectrum for the formation of the open-structured members **12-14** after 2 hours of the reaction is shown in the Supporting Information. Intermediates **12-14** were fully consumed after 2 hours, indicating that they were involved in the construction of macrocycles **9-11**. The unsymmetrical nature of the two different sets of hydrazones in macrocycles **12-14** provides a promising avenue for structural tuning and tailored design, thereby increasing their versatility. It is worth noting that no symmetrical macrocycles were detected by APCI-TOF-MS. This observation suggests that symmetrical macrocycles may form during the early stages of the [2+2]-cyclocondensation reaction, but they undergo remixing to form the more thermodynamically favored unsymmetrical macrocycles. This highlights the importance of reaction conditions and kinetics in determining the final product distribution.

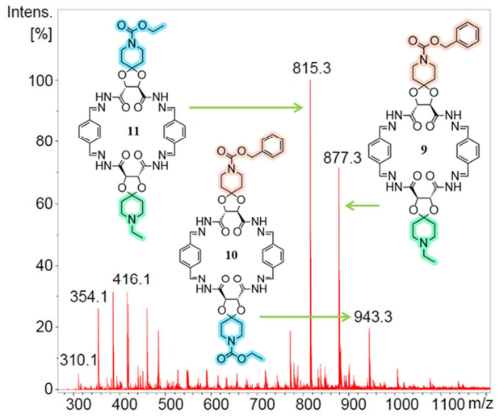

Figure 2. APCI-TOF-MS spectrum of the DCL generated from compounds **3**, **5**, **7**, and **8**.

Following the successful generation of the DCL using terephthalaldehyde **8** in conjunction with **3**, **5**, and **7**, we have determined that further exploration of the DCL is warranted. Thus, we have decided to substitute dialdehyde **8** with 4-(4-formylphenoxy)benzaldehyde **15**. Our objective is to further expand our understanding of the DCL's properties and explore potential variations in its composition. The reaction of dihydrazides **3**, **5**, and **7** with dialdehyde **15** in DMF and MeOH (1: 1) in the presence AcOH under stirring for 24 hours afforded the DCL of macrocycles **16-18** along with the uncyclized compounds **19-22** (**Scheme 2**).

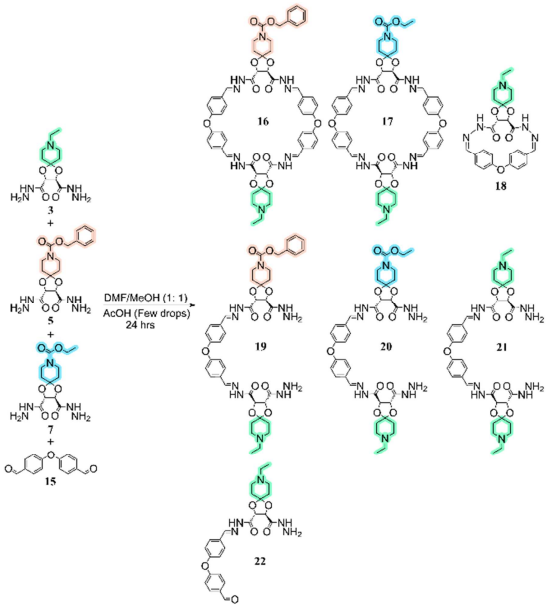

Scheme 3. Generation of a DCL of macrocycle and intermediates **16**-**22**.

The APCI-TOF-MS examination of the DCL produced by reacting dihydrazides **3**, **5**, and **7** with dialdehyde **15** demonstrated the generation of macrocycles **16**, **17**, and **18**, which had corresponding *m/z* values of 1061.4264, 999.3995, and 478.2085. The characteristic peaks of the uncyclized derivatives **19**, **20**, **21**, and **22** appeared in the MS spectra at *m/z* 871.3733, 809.3577, 765.3678, and 496.2191 (See **Table 2**, **Figure 3**, and the Supporting Information). After 24 hours of the reaction, non-symmetric macrocycles were identified, and no symmetric macrocycles were detected. This observation suggests that the non-symmetric macrocycles could be the thermodynamically favored products.

Table 2. APCI-TOF-MS data of the DCL members in the positive ion mode

Entry	Molecular Formula	Calcd. *m/z*	Meas. *m/z*		Error ppm
16[a]	$C_{56}H_{56}N_{10}O_{12}$	1061.4227	1061.4264	$[M+H]^+$	+3.6
17[a]	$C_{51}H_{54}N_{10}O_{12}$	999.4043	999.3995	$[M+H]^+$	–4.7
18[b]	$C_{25}H_{27}N_5O_5$	478.2091	478.2085	$[M+H]^+$	–1.4
19[a]	$C_{42}H_{50}N_{10}O_{11}$	871.3749	871.3733	$[M+H]^+$	–1.8
20[a]	$C_{37}H_{48}N_{10}O_{11}$	809.3587	809.3577	$[M+H]^+$	–1.2
21[a]	$C_{36}H_{48}N_{10}O_9$	765.3651	765.3678	$[M+H]^+$	+3.6
22[b]	$C_{25}H_{29}N_5O_6$	496.2172	496.2191	$[M+H]^+$	–1.4

[a]Detected after 24 hours and [b]detected after 2 hours of stirring at room temperature

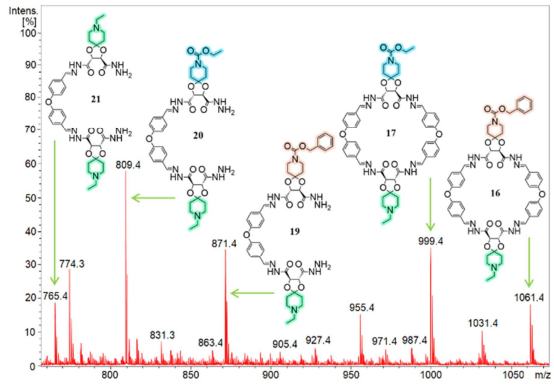

Figure 3. APCI-TOF-MS spectrum of the DCL generated from compounds **3**, **5**, **7**, and **15**.

Based on the APCI-TOF-MS data (**Figures 2** and **3**), the condensation reaction occurs *via* a stepwise reaction mechanism. The reaction initiates with the condensation of one molecule of dihydrazide with one molecule of dialdehyde, which generates (**A**). Subsequently, (**A**) reacts with another molecule of dihydrazide to afford (**B**) and then reacts with another molecule of dialdehyde to yield (**C**). It's noteworthy that the uncyclized product (**D**) which possesses two terminal formyl groups was not detected in any of the measured MS spectra (**Figure 4**).

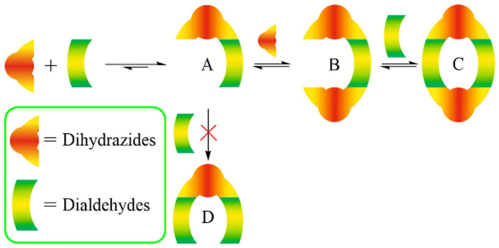

Figure 4. Graphical illustration of the proposed mechanism of the [2+2]-cyclocondensation reactions.

Molecular Modeling

To gain a deeper understanding of the conformational structures exhibited by the DCLs, we employed HyperChem software release 8.0.10 to conduct molecular modeling simulations [20]. These simulations, based on molecular mechanics (MM+), allowed us to explore the spatial arrangements and energetics of the generated DCL constituents. **Figure 5** illustrates the results of our simulations, with the structures being energy minimized according to the reported X-ray structure by Gawroński *et al.* [17] (See supporting information).

Our analysis of the DCL members' lowest energy structures yielded intriguing findings. Notably, we observed the presence of four amide bonds within the optimized structure, with two adopting a *cis*-orientation and the remaining two adopting a *trans*-orientation. This configuration of the amide bonds plays a crucial role in the overall stability and dynamic behavior of the DCLs.

In addition to the *cis* and *trans* amide bonds, our observations revealed that the macrocycles and intermediates exhibited distinct bending structures. This flexibility and adaptability of the structures suggest their potential utility in various applications, particularly in the field of molecular recognition. The bending structures of the molecules enable optimal positioning of functional groups, facilitating efficient interactions with specific target molecules.

Furthermore, our investigation unveiled an interesting phenomenon within the DCLs. Specifically; we observed that the terminal hydrazides of the intermediates were in close proximity to each other, thereby facilitating facile macrocyclization. This proximity enhances the

likelihood of intramolecular reactions, leading to the formation of larger macrocyclic structures. Our comprehensive analysis using molecular modeling simulations has provided valuable insights into the conformational diversity and potential functionalities of the DCLs. The observed bending structures, along with the possibility of template amplification, underscore the promising nature of these dynamic libraries and their potential to advance molecular recognition and materials discovery.

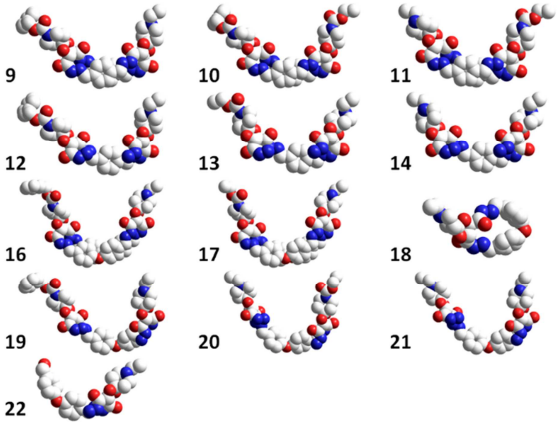

Figure 5. Energy minimized structures of the DCL constituents **9**-**14** and **16**-**22** by molecular mechanics MM+. Hydrogen atoms were omitted for clarity.

3. Experimental

Materials and Methods

All the reagents used for the reactions were purchased from Sigma-Aldrich, AppliChem or Flucka (Germany) and were used as obtained without further purification. Whenever possible the reactions were monitored by thin layer chromatography (TLC). TLC was performed on Macherey-Nagel aluminium-backed plates pre-coated with silica gel 60 (UV_{254}). ^1H and ^{13}C NMR spectra were acquired on a JEOL ECX-400 spectrometer operating at 400 MHz for ^1H NMR and 100 MHz for ^{13}C NMR in DMSO-d_6 using a 5 mm probe. The chemical shifts (δ) were reported in parts per million (ppm) and referenced to the residual solvent peak. The following abbreviations are used: brs, broad singlet; m, multiplet. Mass spectra were recorded using Bruker HCTultra and high resolution Bruker Daltonics micrOTOF instruments from DMF, MeOH, $CHCl_3$, CH_3CN, or water using the positive or negative ion modes. Calibration was carried out using a 0.1 M solution of sodium formate in the enhanced quadratic mode prior to each experimental run. The results of measurements were processed by Compass 1.3 software for a Bruker Daltonics TOF mass spectrometer. Molecular modeling simulations were carried out using HyperChem software release 8.0.10. The structures were energy-minimized using the molecular mechanism (MM+) method. The structures were energy minimized based on of the reported X-ray structure by Gawroński and coworkers [17]. Dihydrazide **7** was synthesized following the experimental procedure reported in literature [19].

General procedures for the synthesis of dihydrazides 3, 5 and 7

To a stirred solution of (+)-diethyl *L*-tartrate **2** (37.17 mmol) in EtOAc (50 mL) were added 1-ethylpiperidin-4-one **1**, benzyl 4-oxopiperidine-1-carboxylate **4** or ethyl 4-oxopiperidine-1-carboxylate **6** (37.16 mmol) and boron trifluoride–diethyl ether (92.9 mmol). The reaction mixture was refluxed for 7 hours, then cooled to room temperature, carefully quenched with $NaHCO_3$ solution (100 mL), extracted with H_2O, dried with anhydrous Na_2SO_4, filtered, and the solvent was evaporated under reduced pressure. The crude oil was dissolved without purification in absolute ethanol (40 mL) and hydrazine monohydrate was added in excess. The mixture was refluxed for 7 hours, the solvent was evaporated under reduced pressure, and the residue was dissolved in water and extracted with ethyl acetate (3×100 mL). The water extract was dissolved in EtOH, dried and evaporated under reduced pressure to afford the title products.

(2*R*,3*R*)-8-Ethyl-1,4-dioxa-8-azaspiro[4.5]decane-2,3-dicarbohydrazide 3

The dihydrazide was obtained as yellow oil (45%). ^1H NMR (400 MHz, DMSO-d_6) δ = 9.3 (brs, 2H, N*H*), 4.4 (brs, 2H, C*H*), 3.7-4.3 (brs, 4H, NH_2), 2.2-2.5 (m, 6H, CH_2), 1.6-1.8 (m, 4H, CH_2), 0.9 (m, 3H, CH_3) ppm. ^{13}C NMR (100 MHz, DMSO-d_6) δ = 167.7, 111.3, 76.9, 51.6, 50.6, 35.5, 12.8 ppm. TOF-MS (+ve ion mode, Molecular Formula, $C_{11}H_{21}N_5O_4$), *m/z* (Calcd. 310.1486, measured, 310.1474 $[M+Na]^+$, error = 3.7).

Benzyl (2*R*,3*R*)-2,3-di(hydrazinecarbonyl)-1,4-dioxa-8-azaspiro[4.5]decane-8-carboxylate 5

The dihydrazide was obtained as yellow oil (40%). ^1H NMR (400 MHz, DMSO-d_6) δ = 9.1 (brs, 2H, N*H*), 7.2-7.4 (m, 5H, Ar*H*), 5.0 (brs, 2H, CH_2), 4.5 (brs, 2H, C*H*) 3.9-4.3 (brs, 4H, NH_2), 3.3-3.6 (m, 4H, CH_2) 1.5-1.8 (m, 4H, CH_2) ppm. ^{13}C NMR (100 MHz, DMSO-d_6) δ = 167.6, 154.8, 137.4, 128.9, 128.3, 128.0, 110.8, 76.9, 66.8, 44.2, 42.0 ppm. TOF-

MS (+ve ion mode, Molecular Formula, $C_{17}H_{23}N_5NaO_6$), *m/z* (Calcd. 416.1541, measured, 416.1556 $[M+Na]^+$, error = −3.6).

Ethyl (2*R*,3*R*)-2,3-di(hydrazinecarbonyl)-1,4-dioxa-8-azaspiro[4.5]decane-8-carboxylate 7

The dihydrazide was obtained as yellow gummy substance according to the reported method [19] (46%). ^{1}H NMR (400 MHz, DMSO-d_6) δ = 1.3 (t, CH_3, 3H), 1.5-1.7 (m, CH_2, 4H), 3.3-3.4 (m, CH_2, 4H), 3.9-4.0 (q, CH_2, 2H), 3.4 (brs, NH_2, 4H), 4.4 (brs, C*H*, 2H), 9.3 (brs, N*H*, 2H) ppm. ^{13}C NMR (100 MHz, DMSO-d_6) δ = 15.0, 35.4, 41.8, 61.3, 77.2, 110.9, 155.0, 167.6 ppm. TOF-MS (−ve ion mode, Molecular Formula, $C_{12}H_{21}N_5O_6$), *m/z* (Calcd. 330.1436, measured, 330.1419, error = −3.6).

Synthetic method of the DCLs 9-11 and 12-14

Dihydrazides **3**, **5**, and **7** (0.30 mmol) were mixed with dialdehydes **8** or **15** (0.90 mmol) in a solvent mixture of DMF and MeOH (1: 1, 4 mL of each solvent). Few drops of AcOH were added to catalyze the condensation reaction and the mixture was stirred at room temperature for 46 or 24 hours. Aliquots from the reaction mixture were taken and dissolved in DMF, MeOH, and $CHCl_3$. The samples were sonicated and analyzed with the high resolution TOF-MS instrument in the positive ion mode.

4. Conclusion

DCC is a powerful approach for generating diverse and complex molecular architectures. We successfully employed DCC to generate macrocycles and intermediates with unprecedented diversity. We prepared the DCLs by reacting three different dihydrazide precursors with two different dialdehydes, resulting in a large number of structurally diverse products. To verify the structures of the DCLs, we utilized direct injection TOF-MS with APCI detection, which proved to be a highly versatile and precise analytical tool for analyzing complex mixtures of products. The mass spectrometry data allowed us to confirm the structures of the DCLs and to deduce the mechanism of the macrocyclization reaction. In addition to mass spectrometry, we also conducted a molecular modeling study to investigate the conformational structures of the DCL members. Our simulations revealed interesting insights into the nature of the amide bonds and the bending structures of the macrocycles, which could be significant for tuning their molecular recognition properties. Our results highlight the potential of DCC as a versatile methodology for generating complex molecular architectures, and the utility of mass spectrometry in elucidating the structures of the DCL members.

5. Conflicts of interest

"There are no conflicts to declare".

6. References

[1] J. Li, P. Nowak, S. Otto, Dynamic combinatorial libraries: from exploring molecular recognition to systems chemistry, J. Am. Chem. Soc., 135, (2013), 9222–9239.

[2] P.T. Corbett, J. Leclaire, L. Vial, K.R. West, J.L. Wietor, J.K. Sanders, S. Otto, Dynamic combinatorial chemistry, Chem. Rev., 106, (2006), 3652–3711.

[3] S. Otto, R.L. Furlan, J.K. Sanders, Dynamic combinatorial chemistry, Drug. Discov. Today, 7, (2002), 117–125.

[4] A. Canal-Martin, R. Perez-Fernandez, Protein-directed dynamic combinatorial Chemistry: An efficient strategy in drug design, ACS Omega**,** 5, (2020), 26307–26315.

[5] G.R.L. Cousins, R.L.E. Furlan, Y.F. Ng, J.E. Redman, J.K.M. Sanders, Identification and isolation of a receptor for *N*-methyl alkylammonium salts: Molecular amplification in a pseudo-peptide dynamic combinatorial library, Angew. Chem. Int. Ed. Engl., 40, (2001), 423–428.

[6] K. Ziach, A. Obrocka-Hrycyna, J. Jurczak, Dynamic combinatorial libraries of 2,5-diformylfuran-derived macrocycles, J. Org. Chem., 79, (2014), 10334–10341.

[7] S.H. Hewitt, A.J. Wilson, Generation of dynamic combinatorial libraries using hydrazone-functionalized surface mimetics, Eur. J. Org. Chem., 2018, (2018), 1872–1879.

[8] A.G. Ekstrom, J.T. Wang, J. Bella, D.J. Campopiano, Non-invasive ^{19}F NMR analysis of a protein-templated *N*-acylhydrazone dynamic combinatorial library, Org. Biomol. Chem., 16, (2018), 8144–8149.

[9] M. Dumartin, J. Septavaux, M. Donnier-Marechal, E. Jeamet, E. Dumont, F. Perret, L. Vial, J. Leclaire, The dark side of disulfide-based dynamic combinatorial chemistry, Chem. Sci., 11, (2020), 8151–8156.

[10] S. Zhao, Y. Wu, L. Hu, Identification and synthesis of selective cholesterol esterase inhibitor using dynamic combinatorial chemistry, Bioorg. Chem., 119, (2022), 105520.

[11] J. Xu, S. Zhao, S. Zhang, J. Pei, Y. Li, Y. Zhang, X. He, L. Hu, Development of a multivalent acetylcholinesterase inhibitor via dynamic combinatorial chemistry, Int. J. Biol. Macromol., 150, (2020), 1184–1191.

[12] Y. Wu, S. Zhao, C. Liu, L. Hu, Development of urease inhibitors by fragment-based dynamic combinatorial chemistry, ChemMedChem, 17, (2022), e202200307.

[13] Y. Wu, S. Zhao, L. Hu, Identification of potent alpha-amylase inhibitors *via* dynamic combinatorial chemistry, Bioorg. Med. Chem., 55, (2022), 116609.

[14] R.P. Jumde, M. Guardigni, R.M. Gierse, A. Alhayek, D. Zhu, Z. Hamid, S. Johannsen, W.A.M. Elgaher, P.J. Neusens, C. Nehls, J. Haupenthal, N. Reiling, A.K.H. Hirsch, Hit-optimization using target-directed dynamic combinatorial chemistry: Development of inhibitors of the anti-infective target 1-deoxy-*d*-xylulose-5-phosphate synthase, Chem. Sci., 12, (2021), 7775–7785.
[15] G. Bagnolini, B. Balboni, F. Schipani, D. Gioia, M. Veronesi, F. De Franco, C. Kaya, R.P. Jumde, J.A. Ortega, S. Girotto, A.K.H. Hirsch, M. Roberti, A. Cavalli, Identification of RAD51-BRCA2 inhibitors using *N*-Acylhydrazone-based dynamic combinatorial chemistry, ACS Med. Chem. Lett.**,** 13, (2022), 1262–1269.
[16] D. Carbajo, Y. Perez, J. Bujons, I. Alfonso, Live-cell-templated dynamic combinatorial chemistry, Angew. Chem. Int. Ed., 59, (2020), 17202–17206.
[17] P. Skowronek, M. Kuncewicz, M. Brzostowska, A. Janiak, U. Rychlewska, J. Gawroński, An expedient synthesis and conformational features of acylhydrazone macrocycles derived from tartaric acid: Evidence of water and π aromatic hydrogen bond interactions, Tetrahedron Asymmetry, 23, (2012), 300–305.
[18] M.C. Misuraca, E. Moulin, Y. Ruff, N. Giuseppone, Experimental and theoretical methods for the analyses of dynamic combinatorial libraries, New J. Chem., 38, (2014), 3336–3349.
[19] H.F. Nour, T. Islam, Fernández-Lahore, M., N. Kuhnert, Probing the dynamic reversibility and generation of dynamic combinatorial libraries in the presence of bacterial model oligopeptides as templating guests of tetra-carbohydrazide macrocycles using electrospray mass spectrometry, Rapid Commun. Mass Spectrom., 26, (2012), 2865–2876.
[20] Molecular Modeling was carried out using HyperChem Software (Release 8.0.10). Trial, version from http://www.hypercubeusa.com/